Submillimeter CO Line Emission from Orion

T. L. Wilson[1,2], D. Muders[1,2], C. Kramer[3], C. Henkel[2]

Received _______________; accepted _______________

[1]Sub-Millimeter Telescope Observatory, Steward Observatory, The University of Arizona, Tucson, Az., 85721

[2]Max Planck Institut für Radioastronomie, Postfach 2024, D-53010 Bonn, Germany

[3]I. Physikalisches Inst., Univ. zu Köln, Zülpicherstr. 77, D-50937 Köln, Germany

ABSTRACT

Images of an 8 square minute region around the Orion KL source have been made in the $J = 7-6$ (806 GHz) and $J = 4-3$ (461 GHz) lines of CO with angular resolutions of $13''$ and $18''$. These data were taken employing on-the-fly mapping and position switching techniques. Our $J = 7-6$ data set is the largest image of Orion with the highest sensitivity and resolution obtained so far in this line. Most of the extended emission arises from a Photon Dominated Region (PDR), but 8% is associated with the Orion ridge. For the prominent Orion KL outflow, we produced ratios of the integrated intensities of our $J = 7-6$ and $4-3$ data to the $J = 2-1$ line of CO. Large Velocity Gradient (LVG) models fit the outflow ratios better than PDR models. The LVG models give H_2 densities of $\sim 10^5$ cm^{-3}. The CO outflow is probably heated by shocks. In the Orion S outflow, the CO line intensities are lower than for Orion KL. The $4-3/2-1$ line ratio is 1.3 for the blue shifted wing and 0.8 for the red shifted wing. Emission in the jet feature extending $2'$ to the SW of Orion S was detected in the $J = 4-3$ but not the $J = 7-6$ line; the average $4-3/2-1$ line ratio is ~ 1. The line ratios in the Orion S outflow and jet features are consistent with both PDR and LVG models.Comparisons of the intensities of the $J = 7-6$ and $J = 4-3$ lines from the Orion Bar with PDR models show that the ratios exceed predictions by a factor of 2. Either clumping or additional heating by mechanisms, such as shocks, may be the cause of this discrepancy.

1. Introduction

The OMC-1 region is the closest molecular cloud where high mass O-B star formation has recently taken place (see, e.g., the review of O'Dell 2001). The region within $3'$ of Orion KL is a particularly fruitful object of study. There is a chemically rich, dense warm region, the 'Hot Core' (see Wilson et al. 2000 and references therein), two outflow sources (see, e.g., Rodríguez-Franco, Martín-Pintado & Wilson 1999; hereafter RMW, Gaume et al. 1998, McMullin, Mundy & Blake 1993) and extended warm gas from a PDR at the interface with the rear boundary of the Orion H II region. Behind the PDR is the 'Orion ridge'. This is part of the column-like feature extending north-south over 2^o (see, e.g., Tatematsu et al. 1993). Near Orion KL, there is a rapid change in radial velocity in the ridge. This is caused by the presence of a number of separate clouds with different radial velocities (Womack, Ziurys & Sage 1993; Wang, Wouterloot & Wilson 1993). In addition, there is another neutral-ionized gas interface, the Orion Bar, SW of the H II region (see van der Werf et al. 1996).

Spatially extended emission from warm molecular and atomic gas arises in PDR's. In PDR's, the kinetic temperatures reach hundreds of degrees (see Hollenbach & Tielens 1999). Thus the $J = 7-6$ line of CO, emitted from an energy level 156 K above ground, should be a good tracer of molecular gas PDR's. There is a partial map of this region in the $J = 7-6$ line by Howe et al. (1993, $20''$ beam) and a complete map by Schmid- Burgk et al. (1989, $98''$ beam). Schmid-Burgk et al. (1989) used beam switching with chopper throws of $<6'$. Since the CO is more extended, this chopping resulted in confusion between CO emission in the signal and reference beams. Schulz et al. (1995; $15''$ beam) also mapped the Orion KL region in the $J = 4-3$ line of CO, but with a telescope which had a low beam efficiency and from a site closer to sea level. In order to trace the extent of warm gas, to compare CO emission from high and low J rotational levels, and to relate molecular emission to compact

continuum sources (see Mezger, Zylka & Wink 1990, Menten & Reid 1995), we have made position-switched images of the Orion KL region in the $J = 4 - 3$ and $J = 7 - 6$ lines.

2. Observations

The $J = 4 - 3$ and $J = 7 - 6$ line CO data were taken with the 10-meter diameter Heinrich Hertz Telescope (HHT) on Mt. Graham, AZ [4]. At the $J = 4 - 3$ line, at 461.041 GHz, the FWHP beam size is 18″. During the $J = 4 - 3$ and $J = 7 - 6$ line observing sessions, the pointing accuracy, from measurements of Saturn, was better than 2″. Since the pointing model for each receiver is merely a constant offset from a general pointing model, we are confident that the RMS pointing accuracy is 2.5″, the usual value (Wilson et al. 2001). The $J = 4 - 3$ line data were taken on Feb. 3, 1999, Feb. 7, 2000 and Feb. 16, 2001 with a single channel SIS mixer facility instrument at the HHT. The single sideband receiver noise temperature was 260 K. During observations in Feb. 1999, the system noise including corrections for the atmosphere was ∼1200 K; in Feb. 2000 and 2001, the system noise was ∼3500 K. In 1999, we took spectra spaced by one full beam width; these data did not include the Orion Bar feature, and the jet feature SW of Orion S, so in Feb. 2000, we mapped these regions using the On-The-Fly (OTF) technique. All of the OTF maps are fully sampled. The Feb. 2001 data consisted of longer integrations on the red- and blue-shifted maxima in the Orion S outflow. Scans taken toward Orion KL served to calibrate the $4 - 3$ data in all three sessions. Our calibrations were made on the assumption of equal response in the signal and image sidebands. This was checked by a comparison of our peak temperature for the Orion KL, or (0″, 0″) position (Fig. 1(a)) with that of Schulz

[4]The HHT is operated by the Submillimeter Telescope Observatory on behalf of the Max-Planck-Institut f. Radioastronomie and Steward Observatory of the University of Arizona.

et al. (1995). Our peak is 20% lower; given our better beam efficiency and pointing and better weather, we prefer our values.

The chopper wheel calibration provides a corrected antenna temperature, T_A^*, appropriate for a very extended source. At 460 GHz, measurements of the Moon give an efficiency of ∼0.75, while measurements of Saturn (diameter ∼20″) give a main-beam efficiency of ∼0.47; this latter value was used to estimate T_{MB} for compact CO emission, such as from outflow sources. The CO emission from the Orion ridge is very extended NS, but is of limited extent EW. Thus, the appropriate efficiency is that measured for a moderately extended object. For such moderately extended gas, we have no measurements of the HHT efficiencies, so have used the geometric mean of the two measured efficiencies, 0.6, to estimate T_{MB} for quiescent $J = 4 - 3$ CO emission.

The $J = 7 - 6$ line, at 806.652 GHz, was measured on Feb. 12, 1999. The FWHP beam width of the HHT is estimated to be 13″. The pointing at 806 GHz is related to the pointing model by a constant offset, so a check made by measuring the positions of Jupiter and Saturn during the observing run, assured us that the pointing is better than 3″. The data were taken employing the OTF mapping technique with the reference offset by $\Delta\alpha = -15'$, $\Delta\delta = 0'$ from the (0″, 0″) position. The $J = 7 - 6$ line data were taken using Hot Electron Bolometer (HEB) receiver from the Harvard-Smithsonian Center for Astrophysics. The calibration was made using the chopper wheel technique. Tests in the laboratory and at the HHT with a single sideband filter showed no deviations from equal response in the signal and image sidebands. In addition, comparisons with the data of Howe et al. (1993) show excellent agreement. Thus we conclude that the receiver sideband responses are equal. The single sideband receiver noise temperature at the frequency of the $J = 7 - 6$ line was ∼1800 K. During the $J = 7 - 6$ line measurements the average system noise, including corrections for the atmosphere, was ∼14000 K.

The calibration of the CO $J = 7-6$ line is also based on the chopper wheel method. At 806 GHz, measurements of the Moon gave an efficiency of ∼0.75. Measurements of Saturn (diameter ∼20″) and Mars (diameter ≤14″) give a main-beam efficiency of ∼0.40; this value was used to estimate T_{MB} for compact CO emission, such as from outflow sources. For CO emission from the Orion ridge, we have used the geometric mean of the two measured efficiencies, 0.54, to estimate T_{MB}.

The efficiencies obtained from measurements of the planets and Moon indicate that there is some error beam contribution at 806 GHz. This will tend to smooth the spatial distribution of the CO emission. However, none of the extended CO $J = 7-6$ emission is caused by an error beam smearing the intense emission from the Orion KL outflow, since the very extended CO emission features in our map have much smaller line widths and different radial velocities.

The $J = 4-3$ and $J = 7-6$ spectra were analyzed using an Acoustic Optical Spectrometer (AOS) with 1 MHz frequency resolution. At the $J = 4-3$ line rest frequency, the spectrometer resolution is 0.65 km s^{-1}. At the $J = 7-6$ line rest frequency, this is 0.37 km s^{-1}.

To compare our sub-mm data with mm results, we took $J = 2-1$ CO spectra with the HHT in Feb. 2000. At the $2-1$ line frequency, the angular resolution is 33″ and the main-beam efficiency is 0.78. Additional unpublished ^{13}CO $J = 1-0$ and CO $J = 2-1$ data were taken with the IRAM 30-m telescope by R. Mauersberger. The angular resolution of the ^{13}CO data was 21″; the forward and beam efficiencies were 0.91. For CO $J = 2-1$ line data, the beam size was 13″, the forward efficiency was 0.8, and the beam efficiency was 0.45. For the $J = 2-1$ CO data for the Orion KL and Orion S outflows, we have been given access to the data published by RMW.

3. Results

Fig. 1 contains sample spectra. Fig. 2 shows a series of velocity maps and Plate 1 is a color-code brightness plot of T_A^* integrated from -150 km s^{-1} to 150 km s^{-1}. Our CO $J = 4-3$ line for the Orion KL nebula is in Fig. 1(a); the corresponding $J = 7-6$ CO line is in (b).

The extended CO $J = 7-6$ emission has two remarkable properties, best seen in the color plate. First, emission extends over the entire map, that is, warm molecular gas is present over a $\geq 3'$ region. Second, the maximum of the extended emission does *not* peak on the Trapezium, but close to the Orion Ridge. Line parameters for the extended CO emission near the Trapezium are in Fig. 3.

The lowest temperature in our map is 10 K, at (100″, −80″). Near the position of the Trapezium stars, the peak T_A^* is 80 K. The peak T_A^* value of the quiescent CO is $\sim$100 K. This is within 20″ of the (0″, 0″) position. For extended CO $J = 7-6$ emission, the conversion factor from T_A^* to T_{MB} is 1.85. The Planck correction was used to convert a T_{MB} of 185 K to a T_{ex} of 204 K. For extended, optically thick, thermalized emission T_{ex} is equal to the kinetic temperature, T_{kin}. Since the CO has small scale clumping (next section), T_{kin} is actually larger than the peak CO temperature. We discuss CO emission at the Declination of the Trapezium in the next section.

The well known, prominent Orion KL outflow is near our (0″, 0″) offset (see, e.g., RMW). Contour maps of two velocities in the CO outflow toward Orion KL are shown in Fig. 4. We discuss Orion KL in Section 4.2.

Another discrete source is S 6 or Orion S (Batrla et al. 1983, BWB83). This source has the IAU designation '[BWB83] 6'. In maps of sub-mm dust continuum (see Mezger et al. 1990; hereafter MZW) and Far Infrared (FIR) fine structure lines [C II] and [O I]

(Herrmann et al. 1997), the peak intensities of Orion KL and Orion S are comparable, but in the $J = 4-3$ and $7-6$ lines, Orion S is more diffuse and much weaker. The CO emission from Orion S is best seen in our color plate, where we show the locations of a compact outflow (mapped by RMW). The spectra in Fig. 1(c)-(d) were taken toward the blue shifted and red-shifted outflow maxima. We plot the locations of emission from different species in Fig. 5. In the color plate, we show the location of the $\geq 2'$ ($\geq$0.3 pc) long highly collimated jet extending SW (Schmid-Burgk et al. 1990). In Fig. 1(e)-(g) we show spectra from this feature. We discuss Orion S in Section 4.3.

The spectrum in Fig. 1(h) was taken toward the Orion Bar feature; this shows the fit of 2 velocity components; the component at 4 km s^{-1} is not related to the Orion Bar feature. In Fig. 2, at v_{LSR}=9.43 to 12.28 km s^{-1}, the Bar is in the SE. In the color plate and Fig. 2 the Bar appears as two maxima. We show the emission from different species in Fig. 6 and discuss this feature in Section 4.4.

4. Discussion

4.1. The Widespread Quiescent CO $J = 7-6$ Emission

Here we present results and analysis for the extended warm CO emission, concentrating on the Declination of the Trapezium. The CO emission is thought to arise in the interface between the H II region and the molecular cloud, a PDR (see Hollenbach & Tielens 1999). The most prolific sources of UV radiation is the star θ^1 C Orionis, the brightest star in the Trapezium. If only the Trapezium heated the CO, and the geometry were plane parallel, one would expect the warm CO emission to peak at the location of θ^1 C. From plate 1, this is definitely *not* the case. Stacey et al. (1993) proposed that θ^1 C is located in a cavity in the molecular cloud. This proposal would reduce the amount of emission from the PDR

toward θ^1 C, but does *not* explain the east-west asymmetry in this emission.

To make a quantitative relation between the CO $J = 7-6$ emission and the Trapezium stars, we plot parameters of CO line profiles at the Declination of θ^1C, at $\Delta\delta = -53''$. Given our high angular resolution, this offset allows us to avoid emission from the discrete sources Orion KL and Orion S. In Fig. 3, we show gaussian fit parameters for the CO profiles. Relative to the R. A. of θ^1C, all of the CO maxima are at $\Delta\alpha = -33''$ to $-38''$, close to the location of the Orion ridge. The warmer ($J = 7-6$) CO peaks $5''$ east of the cooler ($J = 2-1$) CO. The column density of ^{13}CO peaks $9''$ west of the warm CO and $4''$ west of the cooler CO. The warmer CO is found closer to θ^1C. The offset of the CO $J = 7-6$ line relative to $J = 2-1$ line is small, but given the pointing accuracy, is significant. Since the warmer CO is offset in the direction of the Trapezium, we conclude that some of the CO in the Orion ridge is heated by the Trapezium stars.

We use the $J = 7-6$ temperatures in Fig. 3 to estimate the proportion of warm molecular gas in the PDR and Orion ridge at this Declination. We drew a smooth curve connecting $\Delta\alpha = 100''$ with $-200''$; the area above this is the emission from the Orion ridge. The ratio of areas in the Orion ridge to that between $400''$ and $-300''$ is 0.08. On this basis, 92% of the warm molecular gas arises in the PDR, the remainder in the Orion ridge. Since there is no counterpart of the Orion ridge in maps of ionized gas (see, e.g., Wilson et al. 1997), we conclude that lower mass stars heat this gas. According to Hillenbrand & Hartmann (1998) there are about 4500 $M_\odot$ in stars within $12'$ of the Trapezium, so there would be sufficient stars to provide heating in this part of the Orion ridge. According to Kaufman, Hollenbach & Tielens (1998), embedded stars would be the most efficient heating sources.

From PDR models and measured CO line intensities, we determine a range of H_2 densities. We assume that the region is illuminated from one side only. From Model B

(Fig. 10a) of Köster et al. (1994; KSSS) the best agreement with data is for a density of $\sim 10^6$ cm^{-3}. This is true for a range of radiation fields. A more recent PDR model, by Kaufman et al. (1999; KWHL) also allows estimates of H_2 densities from the ratio of the CO $J = 6 - 5$ to $J = 1 - 0$ lines. From interpolation, we obtain a density of 10^5 cm^{-3}. We take this density as the best estimate. Toward the Trapezium, Rodríguez-Franco et al. (2001) found a density of 2 10^6 cm^{-3} from a multi-transition analysis of CN data.

In PDR's, one expects strong emission from [C II] and [O I], so we have plotted the integrated line intensities (from Herrmann et al. 1997) in Fig. 3(d); the maps have angular resolutions of $\sim 1'$, which leads to some confusion in a region as complex as Orion. However, the general morphology of the [C II] and [O I] images agree with our warm CO image in the color plate. We have applied the analysis of KWHL to the [C II] and [O I] fine structure line data of Herrmann et al. (1997) to obtain n(H_2)=3 10^4 cm^{-3}, which we take to be the average density. To reconcile the CO, [C II] and [O I] line data, the CO clumps must have a volume filling factor of 0.3. Since we can 'see' the Orion ridge in the optically thick CO $J = 7 - 6$ line the foreground CO in the PDR must be clumped. If the volume filling factor is 0.3, our peak $J = 7 - 6$ Planck temperature, 204 K, becomes a $T_{\rm kin}$ of 680 K. If H_2 densities in the CO emitting region are $> 10^5$ cm^{-3}, the volume filling factor will become smaller and $T_{\rm kin}$ will rise.

We can estimate the total distance from the PDR surface (also referred to as the 'Main Ionization Front' by O'Dell 2001) to the Orion ridge, from our H_2 density of 3 10^4 cm^{-3} and PDR models. A general prediction of PDR models is that substantial heating extends to a visual extinction, $A_{\rm v}$, of 10 magnitudes, or a column density of 10^{22} cm^{-2}. Given the average H_2 density, we have a good estimate of the *total* distance from the ridge to the PDR interface which will not be affected by clumping. Using 3 10^4 cm^{-3}, the *total* distance is 3 10^{17} cm or 0.1 pc. If H_2 densities in the CO emitting region are larger, this is

an *upper* limit to the line-of-sight distance. Since the Trapezium is 0.25 pc in front the of the PDR interface/Main Ionization Front (see O'Dell 2001), the total distance from θ^1C to the Orion ridge must be $\leq$0.35 pc, but in no case less than 0.27 pc. Rodríguez- Franco, A., Martín-Pintado, J. & Fuente, A. (1998) also favor a small line-of-sight distance between the Orion ridge and PDR on the basis of HC_3N and CN kinematics.

4.2. The Orion KL outflow

This source is prominent in our images because of the energetic CO outflow. Most likely, the region driving the energetic CO outflow is a heavily obscured compact radio continuum source (Churchwell et al. 1987; Garay, Moran & Reid 1987 (GMR)), which coincides with the SiO maser center (Menten & Reid 1995 (MR)). In the IAU classification, this source is '[GMR] B' or '[MR95c] I'; the most commonly used name is source 'I'. We show an image of the CO $J = 7-6$ integrated intensities for a typical range of red and blue shifted velocities in Fig. 4. The position and overall distribution of the emission is very similar to that found in the $J = 2-1$ line emission maps of RMW. As found for lower J CO lines, the line connecting the blue and red shifted maxima passes 10$''$ north of (0$''$, 0$''$) in Fig. 2, the position of source 'I'. A comparison of the $J = 2-1$ emission with the $J = 7-6$ data shows that the $7-6$ emission has more structure. The critical density needed to populate the $J = 7$ level is $\sim 10^6$ cm^{-3}, 43 times larger than for the $J = 2$ level. Thus we conclude that these differences are caused by line excitation effects.

In Table 1, we list integrated CO intensities for selected velocity intervals (Col. 3 and 4) and also ratios of integrated line intensities of the $J = 7-6$ and $J = 4-3$ lines to the $J = 2-1$ line (Col. 5 and 6). We have chosen the same velocity intervals as those used by RMW to easily compare our data with their $J = 2-1$ line results. The average of the ratios of the sub-mm CO lines to the $J = 2-1$ line is given in Table 1. Trying a number

of different choices of linear or parabolic baselines, we find that the RMS difference in our ratios is $\sim$15%.

The line ratios are very different from LTE ratios for a very warm molecular gas. Given the physical conditions in Orion, Large Velocity Gradient (LVG) models are one approach to determine average densities. We have taken the kinetic temperature in the outflow to be 150 K, and chosen a gradient of 1200 km s^{-1}/pc. The LVG model for an H_2 density of 10^5 cm^{-3}gives ratios of $J = 4 - 3/J = 2 - 1$=2.6 and $J = 7 - 6/J = 4 - 3$=2.3. An alternative is a PDR model. Here a number of additional measurements and assumptions are needed to estimate the H_2 density. The plane-parallel PDR Model A of KSSS describes a region irradiated on both sides. From their Fig. 7(a) for an H_2 density of 10^7 cm^{-3}, the predicted ratios are $J = 4 - 3/J = 2 - 1$=1.6 and $J = 7 - 6/J = 2 - 1$=2.1. The agreement of this prediction with our data is worse than for the LVG model, although the errors are large. On the basis of the average values, we conclude that the LVG model is a better description of the outflow.

There is a significant difference in the source sizes for red (43″) and blue (34″) shifted gas, so we have obtained line ratios by spatially integrating intensities over velocity slices. Also, from Fig. 4, the outflow centers are significantly offset from the (0″, 0″) position. Thus the data collected in Table 6 of Schulz et al. (1995), based on peak temperatures for (0″, 0″) alone, are less accurate.

4.3. Orion S

Compared to Orion KL, this is a prominent source in sub-mm dust emission (MZW), a compact emission region in NH_3 (Batrla et al. 1983), but is less prominent in CO emission, and shows only a few H_2O masers (Gaume et al. 1998). Gaume et al. (1998) detected no

near-IR sources at the center of the H_2O masers, so this source is very deeply embedded. Orion S is hot ($T_{kin} \geq 300$ K) and shows intense [O I] and [C II] emission (Herrmann et al. 1997). There is a low intensity, compact CO outflow. The relative positions of the red and blue shifted maxima are similar to Orion KL (see color plate). From studies of a number of molecular species, McMullin, Mundy & Blake (1993) concluded that the chemistry was consistent with a young region where shock chemistry played the most important role.

In Fig. 1(c) and (d) we show CO $J = 4 - 3$ spectra of the blue- and red- shifted line wings. The outflow spectra are strikingly similar to those in Fig. 2 of RMW. Because of the low line intensities, we have not mapped the outflow regions, but have taken longer integrations at the blue and red shifted maxima. We list the integrated intensities for the two maxima in Table 2. The FWHP beams used to take the $J = 2 - 1$ and $J = 4 - 3$ spectra have similar sizes, so we have formed ratios without corrections for beam or source sizes. From the RMW data, we find that the outflow FWHP sizes are 23$''$ for the red shifted gas and 27$''$ for the blue shifted CO. The ratios for the blue shifted gas are significantly larger than for the red shifted gas. The LVG model for an H_2 density of 7 10^3 cm^{-3} gives a $J = 4 - 3/J = 2 - 1$ ratio of 0.8, while 5 10^4 cm^{-3} gives a ratio of 1.4. The PDR model A of KSSS (Fig. 7(a)) predicts a ratio of $\sim$1 for an H_2 density of 10^5 cm^{-3}. The $J = 7 - 6$ line data had only very short integration times at each position, so were too noisy to allow a detection of the outflow. The difference between the line ratios for Orion KL and Orion S may indicate that PDR conditions play a larger role in Orion S, while the more compact size of Orion S is consistent with a younger source.

In Fig. 5, from high angular resolution data, we show the maxima of different species; except for the H_2O masers, the emission centers are extended by $>10''$. Johnston et al. (1983) found 4 K absorption lines of the 6 cm line of H_2CO over 50$''$ toward Orion S, but no compact continuum source. The 6 cm line of H_2CO usually has T_{ex} <2.7 K, but

the deeper absorption found toward Orion S requires a discrete background source. The observation can be explained if some free-free emission, perhaps from Orion A, were behind the region containing the H_2CO. If the electron density in the ionized gas were 10^4 cm^{-3}, the line-of-sight depth behind the H_2CO absorption region would be $\sim 10^{-3}$ pc. The ionization fronts bordering such a large neutral region inside the Orion A H II region would have been seen in the VLA and HST data of O'Dell & Yusef-Zadeh (2000). Thus there is contradiction which cannot be resolved at this time. The submm CO and FIR results are most easily explained by placing Orion S very close to the PDR interface, where Orion S is exposed to a high UV radiation field. This accounts for the warm dust, high T_{kin}, and a high abundance of atomic oxygen and ionized carbon, but less molecular emission. The offsets of the atomic and molecular maxima are consistent with the major source of ionization arising from the Trapezium. Since Orion S is close to the Orion ridge, the emission is confused and mass estimates are uncertain. Muders & Schmid-Burgk (1992) report the presence of rotation and estimate a mass of 7 $M_\odot$. From their submm dust map, MZW report 65 $M_\odot$; this is very probably an overestimate because of confusion with the ridge.

In Plate 1, we show the position of the jet feature by an arrow. For three positions in the jet we show spectra in Fig. 1 (e)-(g). The $J = 4-3$ to $J = 2-1$ ratios of the integrated T_{MB} values are 1.3, 0.5 and 0.7, respectively. The first two values refer to positions separated by only 15″. The jet feature is at the edge of our $J = 7-6$ map. The nearest position is at an offset ($-40''$, $-150''$), where we find a $J = 7-6$ to $J = 4-3$ ratio of 0.6. Thus, there are large variations in the ratios. Applying an LVG analysis, we obtain an average H_2 density of $\sim 10^4$ cm^{-3}.

4.4. The Orion Bar Feature

The Bar feature is a neutral-ionized gas interface to the SW of Orion KL. This is one of the best studied PDR's and is used for testing PDR models. From Fig. 1(h), the CO emission from the Bar has a radial velocity of $\sim$10.5 km s^{-1}, with a FWHP of $\sim$3.3 km s^{-1}. There is unrelated CO emission at $\sim$4 km s^{-1}. We show a set of radio line measurements in Fig. 6; our data have been produced by integrating intensities from 10 to 11 km s^{-1}. The FWHP of the Orion Bar, measured in the direction of the ionization front (hereafter IF) is 67″. We estimate that the FWHP of the $J = 6-5$ CO emission is $\sim 60''$ from the gray scale plot in Fig. 1 of Lis, Schilke & Keene (1997; LSK). The $J = 6-5$ ^{13}CO data in Fig. 2 of LSK give a FWHP of 30″. In contrast, the CO $J = 1-0$ data of Tauber et al. (1994; TTMG) gives a FWHP of 22″. We plot the $J = 1-0$ data in Fig. 6(b). LSK give only relative coordinates, so we have not used these data in Fig. 6. To reconcile the different FWHP's we assume that the optical depth of the $J = 7-6$ CO emission is $\sim$10 times larger than $J = 1-0$ CO. The $J = 1-0$ maximum of TTMG (1994) is $\sim 5''$ further from the IF than our $J = 7-6$ maximum, and nearly coincident with our $4-3$ peak. Our peak line intensity is T_{MB}=145 K, as is the CO $J = 6-5$ line of LSK, but the peak intensity of the $1-0$ line (TTMG) is 1.5 times smaller.

KSSS have produced PDR models with a plane parallel geometry, illuminated from one side; these are appropriate for the Orion Bar. Their model (Fig. 12) gives the largest $7-6/4-3$ ratio, 1.4. Our observed ratio, $\sim$3.5, is more than twice the model prediction. The PDR model of KWHL may produce slightly higher ratios. It is possible that other mechanisms, such as shock waves, contribute to the heating of the gas in the Bar, or that clumping is a significant factor. In the following, we take the density from the PDR model of KWHL (Fig. 13 and 14), n(H_2) $\sim 10^5$ cm^{-3}. This value seems to be a lower limit, so the higher J lines give H_2 densities which are significantly larger than $\sim 5\,10^4$ cm^{-3}, the value

given by TTMG (1994) and Hogerheijde, Jansen & van Dishoeck (1995).

The best measurement of the FWHP of hot CO emission from the Bar feature is 30″. If the geometry is cylindrical, with an effective diameter of 30″ (=0.073 pc at 500 pc), and length of 100″ (=0.24 pc). Then the mass is 4.6 $M_\odot$. Corrections for clumping would lower this value. For a local density of 10^5 cm^{-3}, the column density of H_2 is 2.2 10^{22} cm^{-2}. The column density agrees with previous values for the Bar, but *requires a cylindrical geometry* not, as commonly thought, a sheet-like region with the long dimension parallel to the line-of-sight (see Fig. 13 of Hogerheijde et al. 1995). Walmsley et al. (2000) have also found evidence for a cylindrical geometry of the Bar from near-IR data.

4.5. Orion Cloud Mass Estimates

To estimate the mass of H_2 over the 8 square minute region mapped in the $J = 7 - 6$ CO line, we will assume that this is a PDR. The heating in PDR's is effective up to a H_2 column density of 10^{22} cm^{-2}. Summing this column density over the region mapped, and including a 10% helium contribution, we find 15 $M_\odot$ of warm molecular gas. Our estimate of this mass does *not* include any contribution from the Orion ridge or Bar.

There have been estimates of the total mass of this region. From measurements of 1.3 mm dust emission, MZW quote a mass of ∼1.7 10^3 $M_\odot$. This estimate depends on (uncertain) dust temperatures and dust properties. We can estimate a more accurate mass between $\Delta\delta = 1'$ and $\Delta\delta = -2'$ using the $J = 2 - 1$ $C^{18}O$ data of White & Sandell (1995) and Eq. 14.115 of Rohlfs & Wilson (1999). The value is ∼310 $M_\odot$. Since the lowest contour in the map is 20 K km s^{-1}, this *must* be a lower limit to the total molecular gas mass. Goldsmith, Lis & Bergin (1997) analyzed the three lowest transitions of $C^{18}O$ for the region between $\Delta\delta = 6'$ and $\Delta\delta = -6'$. Scaling their result to the region of interest, we find a mass

of 420 $M_\odot$. Our value and that of Goldsmith et al. (1997) probably represent the range of molecular mass in denser gas. Then ∼4-5% of the total molecular mass is in the form of dense warm molecular gas. As pointed out by a number of authors (see, e.g., Wilson et al. 1997) the mass of ionized gas in Orion A is $\ll$10 $M_\odot$. Taking the estimates in Hillenbrand & Hartmann (1999), we find 1200 $M_\odot$ of stars within 1.2′ of θ^1C. Thus, the mass in stars dominates.

5. Summary

We have mapped an 8 square arcmin region in the $J = 7-6$ and $J = 4-3$ lines of CO. We summarize the properties of individual CO emission features in Table 3. From our sub-mm CO data and published results, we find that:

1. The $J = 7-6$ quiescent CO emission is present over the entire region mapped. The gas is quiescent with $\Delta V_{1/2}$=4 to 6 km s^{-1}. Our data, together with PDR model calculations of KWHL, show that the $J = 4-3$ and $J = 7-6$ CO emission is consistent with an H_2 density of 10^5 cm^{-3}. The neutral-ionized gas interface has a depth of ∼3 10^{17} cm. The mass of warm molecular gas in the H II region– molecular cloud interface which we mapped in the $J = 7-6$ line of CO is 15 $M_\odot$.

2. The warm CO emission peaks west of the position of the Trapezium star, θ^1 C. There is a difference in the positions of the CO, with $J = 7-6$ CO 33″ peaking west of the position of θ^1 C. The $J = 2-1$ CO is 5″ west of the $J = 7-6$ maximum, and ^{13}CO 9″ west of the $J = 7-6$ peak. From the differences in peak position, we conclude that the CO $J = 7-6$ emission toward the Orion ridge is partly heated by Trapezium stars. Embedded stars may provide the rest of the heating.

3. From a PDR analysis of CO and atomic fine structure [C II] and [O I] line data, the *total*

distance of Orion ridge from the H II region- molecular cloud interface is 3 10^{17} cm. Since the projected distance is 2.8 10^{17} cm, the line-of-sight distance is 10^{17} cm. The CO emission arises from clumps with a volume filling factor 0.3. From the filling factor and maximum Planck temperature of 204 K, the maximum value of T_{kin} is 680 K. If H_2 densities in the CO emitting region are $> 10^5$ cm^{-3}, the volume filling factor and line-of-sight distance will be smaller and T_{kin} will rise.

4. The ratios of $J = 7-6$ to $J = 4-3$ and $J = 4-3$ to $J = 2-1$ in the Orion KL outflow are ∼2. As with the $J = 2-1$ CO, the line connecting the largest peaks in the outflow is $10''$ north of the position of source 'I', which is thought to be the driving source (MR). From an LVG analysis, the H_2 density in the Orion KL outflow is $\sim 10^5$ cm^{-3}.

5. The Orion S region has high T_{kin} and large abundance of atomic species are most simply explained by assuming that this region is younger than Orion KL and very close to the PDR interface at the back face of the H II region Orion A.

6. The ratio of the $J = 4-3$ to $J = 2-1$ lines in the Orion S outflow is significantly larger for blue shifted CO. The ratios are lower than the ratios found for Orion KL. In an LVG model, the H_2 densities are 7 10^3 cm^{-3} for the red shifted CO and 5 10^4 cm^{-3} for the blue shifted CO. From a PDR analysis, the H_2 density would be 10^5 cm^{-3}.

7. For the highly collimated jet-like feature extending SW of Orion S, we have measured $J = 4-3$ to $J = 2-1$ ratios at 3 positions. The average value is unity. An LVG analysis gives an H_2 density of $\sim 10^4$ cm^{-3}. 8. Our $J = 7-6$ to $4-3$ line ratio for the Orion Bar is ~ 3.5, larger than the highest value predicted by PDR models. We take the H_2 density for this region to be $\geq 10^5$ cm^{-3}. From this density and measured sizes, the mass is 4.5 $M_\odot$ Given this density, the geometry must be cylindrical, not a sheet-like geometry, to match the generally accepted column density of $\sim 10^{22}$ cm^{-2}.

9. From an analysis of $C^{18}O$ $J = 2-1$ line emission data, the total mass of gas in the region mapped is between 310 and 420 $M_\odot$. Based on PDR models, the mass of warm molecular gas in the PDR interface is 15 $M_\odot$, while the mass in ionized gas is $\ll$10 $M_\odot$, and mass of stars in this region is 1200 $M_\odot$.

Acknowledgements We thank the Sub-mm Array Receiver Group at the Harvard-Smithsonian Center for Astrophysics for providing the HEB receiver. We also thank the SMTO staff, especially M. Dumke, for help with the observations. R. Mauersberger and A. Rodríguez-Franco provided data in a digital form. W. Fusshoeller helped to prepare some of the figures. An anonymous referee and Prof C. R. O'Dell helped to improve the text.

REFERENCES

Batrla, W., Wilson, T. L., Bastien, P. & Ruf, K. 1983 A & A 128, 279

Churchwell, E., Felli, M., Wood, D. O. S., & Massi, M. 1987 ApJ 321, 516

Garay, G., Moran, J. M. & Reid, M. 1987 ApJ 314, 535

Gaume, R.A., Wilson, T.L., Vrba, F.J., Johnston, K.J. & Schmid-Burgk, J. 1998, ApJ 493, 940

Goldsmith, P. F., Bergin, E.A. & Lis, D.C. 1997 ApJ 491, 615

Hollenbach, D. J. & Tielens, A. G. G. M. 1999 Rev. Mod. Phys. 71, 173

Herrmann, F. et al. 1997 ApJ 481, 343

Hillenbrand, L. & Hartmann, L. W. 1998 ApJ 492, 540

Howe, J. E., Jaffe, D. T., Grossman, E. N., Wall, W. F., Mangum, J. G., Stacy, G. J. 1993 ApJ 410, 179

Hogerheijde, M. R., Jansen, D. J. & van Dishoeck, E. F. 1995 A & A 294, 792

Johnston, K. J., Gaume, R. A., Wilson, T. L., Nguyen, H. A. & Nedoluha, G. E. 1997, ApJ 490, 758

Johnston, K. J., Palmer, P., Wilson, T. L. & Bieging, J. H. 1983, ApJ 271, L89

Kaufman, M. J., Hollenbach, D. J. & Tielens, A. G. G. M. 1998 ApJ 497, 276

Kaufman, M. J., Wolfire, M. G., Hollenbach, D. J. & Luhman, M. L. 1999 ApJ 527, 795 (KWHL)

Köster, B., Störzer, H., Stutzki, J.& Sternberg, A. 1994 A & A 284, 545 (KSSS)

Lis, D. C., Schilke, P., Keene, J. 1997 in ‘CO: 25 Years of Millimeter Wave Spectroscopy’ ed. W. B. Latter, S. J. E. Radford, P. R. Jewell, J. G. Mangum & J. Bally (Kluwer, Dordrecht), p. 128

McMullin, J. P., Mundy, L. G. & Blake, G. A. 1993 ApJ 405, 599

Menten, K. M. & Reid, M. J. 1995 ApJ 445, L157 (MR)

Mezger, P. G., Zylka, R. & Wink, J. 1990 A & A 228, 95 (MZW)

Mundy, L. G., Scoville, N. Z., Baath, L. B., Masson, C. R. & Woody, D.P. 1986, ApJ 304, L51

Muders, D. & Schmid-Burgk, J. 1992 in Astronomische Gesellschaft Abstract Series No. 7, E12

O’Dell, C. R. & Yusef-Zadeh, F. 2000 AJ 120 382

O’Dell, C. R. 2001 ARAA (in press)

Rohlfs, K. & Wilson, T. L. 1999 ‘Tools of Radio Astronomy’, 3rd edition, Springer-Verlag, Heidelberg

Rodríguez-Franco, A., Martín-Pintado, J. & Fuente, A. 1998 A & A 329, 1097

Rodríguez-Franco, A., Martín-Pintado, J. & Wilson, T. L. 1999 A & A 344, L57 (RMW)

Rodríguez-Franco, A., Wilson, T. L., Martín-Pintado, J. & Fuente, A. 2001 A & A (submitted)

Schulz, A. et al. 1995 A & A 295, 183

Schmid-Burgk, J. et al. 1989 A & A 215, 150

Schmid-Burgk, J., Güsten, R., Mauersberger, R., Schulz, A. & Wilson, T.L. 1990 ApJ 362, L25

Simon, R., Stutzki, J., Sternberg, A. & Winnewisser, G. 1997 A&A 327, L9

Stacey, G. J., Jaffe, D. T., Geis, N., Genzel, R., Harris, A. I., Poglitsch, A. Stutzki, J. & Townes, C. H. 1993 ApJ 404, 219

Störzer, H., Stutzki, J. & Sternberg, A. 1995 A & A 296, L9

Tatematsu, K. et al. 1993 ApJ 404, 643

Tauber, J. A., Tielens, A. G. G. M., Meixner, M. & Goldsmith, P. F. 1994 ApJ 422, 136 (TTMG)

Tauber, J. A., Lis, D. C., Keene, J., Schilke, P. & Büttgenbach, T. H. 1995 A & A 297, 567

Walmsley, C. M. Natta, A., Oliva, E., Testi, L. 2000 A & A 303, 544

Wang, T. Y., Wouterloot, J. G. A. & Wilson, T. L. 1993 A & A 277, 205

Werf, P.P. van der, Stutzki, J., Sternberg, A., Krabbe, A. 1996 A & A 313, 633

White, G. & Sandell, G. 1995 A & A 299, 179

Wilson, T. L., Filges, L., Codella, C., Reich, W., & Reich, P. 1997 A & A 327, 1177

Wilson, T. L., Gaume, R. A., Johnston, K. J. & Gensheimer, P. D. 2000, ApJ 538, 665

Wilson, T. L., Muders, D., Butner, H. M., Gensheimer, P. D., Uchida, K. I., Kramer, C., Tieftrunk, A. R. 2001 'Science with the Atacama Large Array' ed. A. Wootten, PASP (in press)

Womack, M., Ziurys, L. M. & Sage, L. J. 1993 ApJ 406, L29

Wyrowski, F., Schilke, P., Hofner, P. & Walmsley, C. M. 1997 ApJ 487, L171

This manuscript was prepared with the AAS LATEX macros v5.0.

Table 1. High Velocity Line Wing Emission in Orion KL

(1) Velocity Range (km s^{-1})	(2) $J=2-1$ Transition integrated intensity[3] (K · km s^{-1} $''^2$)	(3) $J=4-3$ Transition integrated intensity (K · km s^{-1} $''^2$)	(4) $J=7-6$ Transition integrated intensity (K · km s^{-1} $''^2$)	(5) Ratio[1] of $J=4-3$ to $J=2-1$	(6) Ratio[2] of $J=7-6$ to $J=2-1$
+35 to +55	6.3 10^5	1.1 10^6	2.2 10^6	1.8	3.5
−30 to −50	3.2 10^5	6.8 10^5	9.9 10^5	2.1	3.1
+55 to +75	4.3 10^5	3.6 10^5	7.4 10^5	0.8	1.7
−50 to −70	1.2 10^5	2.8 10^5	3.5 10^5	2.3	2.9
+75 to +95	6.6 10^4	9.0 10^4	6.1 10^4	1.4	0.9
−70 to −90	4.4 10^4	9.9 10^4	5.8 10^4	2.2	1.3
+95 to +115	1.6 10^4	∼8.3 10^4	—	∼5.2	—
−90 to −110	1.6 10^4	∼3.0 10^4	—	∼2.1	—
Average[4]	—	—		2.2±1.3	2.2±1.1

[1] From data in col. 3 and 2.

[2] From data in col. 4 and 2.

[3] Data from RMW

[4] Unweighted average.

Table 2. High Velocity Line Wing Emission in Orion S

(1) Velocity Range (km s^{-1})	(2) $J = 2 - 1$ Transition integrated intensity[(1)] (K · km s^{-1})	(3) $J = 4 - 3$ Transition integrated intensity[(2)] (K · km s^{-1})	(4) Ratio[(3)] of $J = 4 - 3$ to $J = 2 - 1$
+30 to +50	14.5	12.0	0.8
−50 to −20	15.0	14.8	1.0
+50 to +70	19.4	17.2	0.9
−80 to −50	7.1	16.2	2.3

[(1)] Estimated from data of RMW

[(2)] From peak of red and blue shifted outflow profiles (Fig. 1c and d.)

[(3)] From data in col. 3 and 2.

Table 3. Summary of CO Line Results

(1)	(2)	(3)	(4)	(5)
Feature	CO $J = 7 - 6$		Line	H_2
	Maximum	$\Delta v_{1/2}$	Ratio[1]	density
	T_{mb}			$n(H_2)$
	(K)	(km s^{-1})		(cm^{-3})
Quiescent warm gas	150	4–7	~ 1.2	$\geq 10^5$
KL outflow	—		~ 2	10^5
Orion S outflow	—		0.8-1.4[2]	$< 10^4$
Orion S jet	—		~ 1[2]	$\sim 10^4$
Orion Bar	140	3.3	~ 3.5	$> 10^6$

[1] Unless otherwise noted, ratio of $J = 7 - 6$ to $J = 4 - 3$

[2] Ratio of $J = 4 - 3$ to $J = 2 - 1$ lines

Fig. 1.— CO line spectra taken toward various positions. The intensity scale is T_A^*. The offsets (upper right) are with respect to α=05^h 32^m 47^s, $\delta = -05^o\ 24'\ 23''$ (epoch 1950.0). **(a)** The $J = 4-3$ line taken toward the position of IRc2. **(b)** The $J = 7-6$ line taken toward this position. **(c)** The $J = 4-3$ profile at the peak of the blue shifted outflow from Orion S (FWHP resolution 18″). **(d)** The corresponding red shifted outflow from Orion S **(e-g)** A series of line profiles from the jet feature, which extends to the SW of Orion S. In each spectrum, $J = 4-3$ emission is shown as a thin histogram, while the $J = 2-1$ line (taken with the IRAM 30-m telescope, beam 13″) is shown as a thicker smooth line. **(h)** A $J = 4-3$ emission line spectrum from the Bar feature. Superposed is the fit of 2 gaussians: The more intense line at 10.5 km s^{-1} is emitted from the Orion Bar while the weaker line arises from extended unrelated emission.

Fig. 2.— Velocity channel maps of the intensity of the the $J = 7-6$ line of CO. The angular resolution is 13″; the radial velocity, v_{LSR}, is given in the upper left corner of each panel. The units are integrated line intensity in K km s^{-1}, where the temperature is T_A^*; the contour levels are 10 K km s^{-1} to 100 K km s^{-1} in steps of 10 K km s^{-1}. The region in the NE was not mapped. The zero point of the map coordinates is the one given in Fig. 1. The offsets are in arc sec. The prominent feature in the NW part of the map is the Orion KL outflow. The outflow covers a large velocity range, so is present in all the velocity channels shown. The (0″, 0″) position is marked by a '+'; the Orion S outflow is marked by a 'x'. The feature at v_{LSR}=9.43 and 10.85 km s^{-1}, which extends from the Orion KL outflow to the Orion Bar Feature, is also seen in lower resolution maps of FIR fine structure lines of [O I] and [C II] (Herrmann et al. 1997).

Fig. 3.— Plots of gaussian fit parameters for the $J = 7-6$, $4-3$ and $2-1$ lines of CO (from the HHT) as well as the $J = 1-0$ line of ^{13}CO (IRAM 30-m telescope) versus Right Ascension at the Declination of θ^1 C ($\Delta\delta = -53''$). The vertical line through all panels marks the R. A. of the star θ^1 C Orionis. **(a)** The peak temperatures, T_{MB}, for the CO lines. The $J = 7-6$ and $J = 4-3$ T_{MB} values were obtained by multiplying T_A^* values by 1.85 and 1.66, respectively. The conversion factor for other lines is 1.2. Our maximum in the $J = 7-6$ CO line is at $\Delta\alpha = -33''$ while the $J = 2-1$ maximum from 30-m (FWHP $10''$) and HHT (FWHP $33''$) is at $\Delta\alpha = -38''$. The difference between the position of the $J = 2-1$ maximum (representing cooler molecular gas) and $J = 7-6$ maximum (warm gas) is significant. The $C^{18}O$ and ^{13}CO peak at $\Delta\alpha = -42''$, so the column density of CO is west of the warmest CO peak. **(b)** A plot of the FWHP line widths, $\Delta v_{1/2}$, as a function of offset in α. **(c)** A plot of v_{LSR} versus offset in α. **(d)** Atomic fine structure lines from Herrmann et al. (1997; FWHP resolution $\sim 1'$) for the same Declination. The [O I] line data is shown as solid and dashed lines; the [C II] data is shown as a dash dotted line.

Fig. 4.— Plots of the integrated intensities for the Orion KL outflow in the CO $J = 7-6$ line for two velocity intervals, **(a)** the -50 to -70 km s^{-1} velocity range (contours 10, 20, 30, 40, 50, 60, 70, 80 K km s^{-1}) and **(b)** the 55 to 75 km s^{-1} velocity range (contours 10, 30, 50, 70 and 90 K km s^{-1}). The temperatures are T_A^*; multiplying by 2.5 converts these contours to T_{MB}. The star marks the ($0''$, $0''$) position as in Fig. 1. This is the position of source 'I', a 7 mm continuum and SiO maser source. 'I' is considered to be driving the CO outflow (MR). Scanning effects cause the somewhat rectangular shape of the contours.

Fig. 5.— Features associated with Orion S; offsets are relative to our zero point in Fig. 1. There is a compact, high velocity CO outflow (RMW) centered at ($\Delta\alpha$, $\Delta\delta$) = ($-16.5''$, $-85''$); the $J = 4-3$ profiles taken at the maxima for the blue ('B') and red ('R') shifted CO are in Fig. 1(c) and (d). Our $4-3$ emission line peak is rather extended; our average peak position in CO $J = 7-6$ is for v_{LSR}=2.3 to 12.28 km s^{-1} (see Fig. 2). We show the most intense H_2O maser emission center imaged by Gaume et al. (1998) with a $0.1''$ beam. MZW reported the compact 1.3 mm emission region, OMC-1 FIR 4. Within the positional uncertainties of MZW, this is coincident with the H_2O position (Gaume et al. 1998). Mundy et al. (1986) found the CS maximum CS3. The H_2CO absorption toward Orion S (Johnston et al. 1983, resolution $10''$) has a FWHP of $50''$ and a depth of 4 K.

Fig. 6.— Spectral line emission from a number of species in the Orion Bar versus offset from the Ionization Front (IF). **(a)** Data taken along a line with Position Angle 135°, zero point α=05^h 32^m 55.4^s, $\delta = -05^o$ $26'$ $50''$ (1950.0). **(b)** Data taken along lines passing through α=05^h 32^m 52.7^s, $\delta = -05^o$ $26'$ $50''$ and $\delta = -05^o$ $27'$ $00''$ (1950.0), P.A.=135°. Our $J = 7-6$ CO line data are shown as a thick solid line and our $4-3$ data are shown as a thick solid line passing through circles. Both results are in T_A^* units, integrated over a velocity range from 10 to 15 km s^{-1}. The CO $1-0$ data are from TTMG (1994; resolution $7''$). The CN data are from Simon et al. (1997; resolution $14''$). The $J = 5-4$ CS data are from der Werf et al. (1996; resolution $8''$), the $N = 2-1$, $J = 5/2-3/2$ CO^+ data from Störzer, Stutzki & Sternberg (1995; resolution $12''$) and the C I data are from Tauber et al. (1995; resolution $15''$). **(c)** Adapted from Wyrowski et al. (1997); these results are averaged over the width of the Bar feature. The vibrationally excited H_2 data, labelled H_2^*, were taken from van der Werf et al. (1996). The position of the C91α carbon radio recombination line (resolution $11.7''$ by $9.0''$) represents the position of C^+.

Plate 1. A color coded image of the intensity of the $J = 7 - 6$ line of CO, integrated over the velocity range from -150 km s^{-1} to $+150$ km s^{-1}. The intensity scale is shown as a bar on the right side of the map. The angular resolution is $13''$. The zero point of the map coordinates is α=05$^{\rm h}$ 32$^{\rm m}$ 47$^{\rm s}$, $\delta = -05^{\rm o}$ 24$'$ 23$''$ (1950.0). The maxima of the red and blue shifted CO emission in Orion KL and Orion S are marked 'R' and 'B'. The four stars mark the positions of the Trapezium members. The lines with labels '(a)' and '(b)' in the SW are the paths in Fig. 6 (a) and (b). The second Bar peak to the NE was not measured in other species.

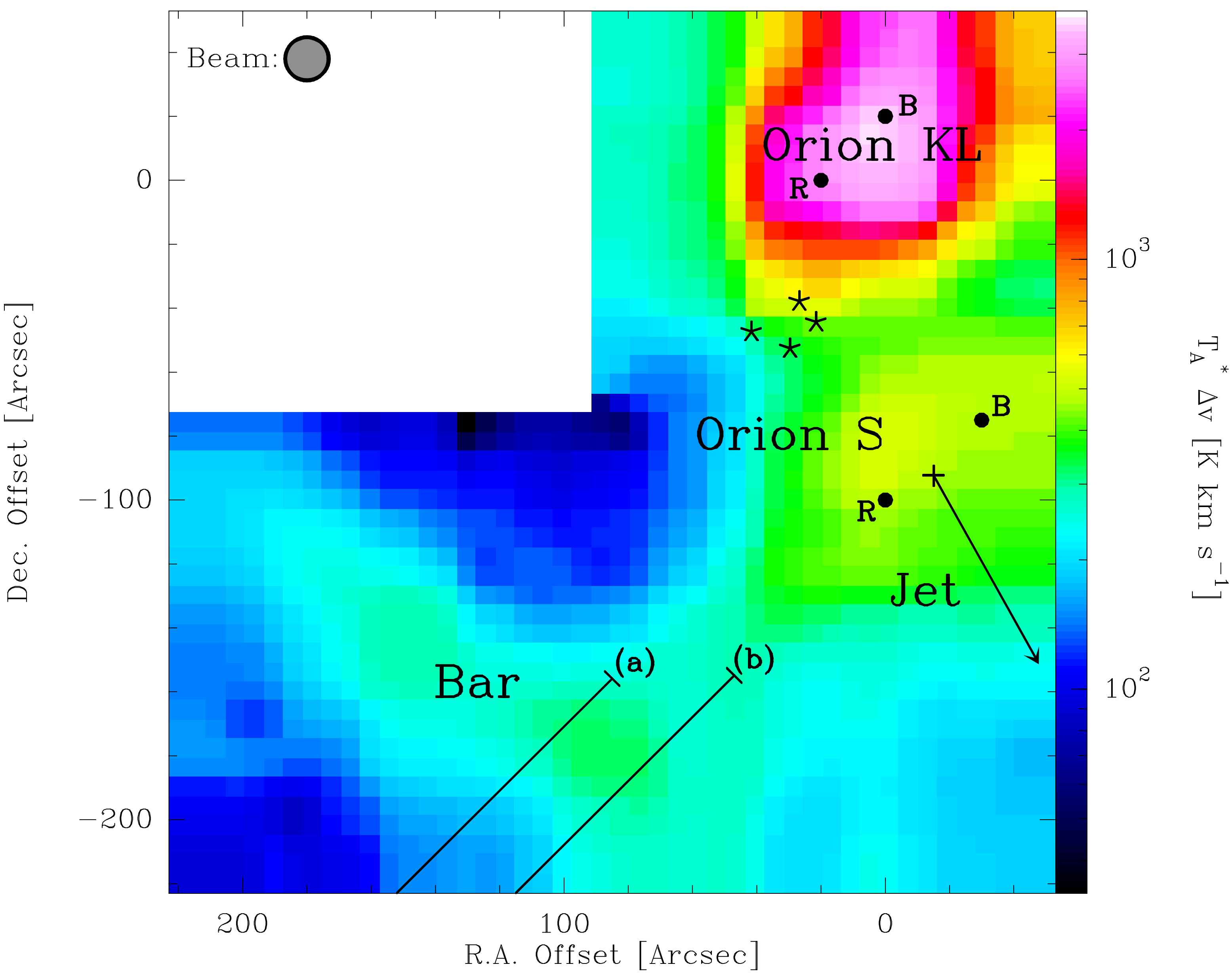

Beam:
Orion KL
B
R
Orion S
B
R
Jet
Bar
(a)
(b)
0
−100
−200
Dec. Offset [Arcsec]
200
100
0
R.A. Offset [Arcsec]
10^3
10^2
$T_A^* \Delta v$ [K km s^{-1}]

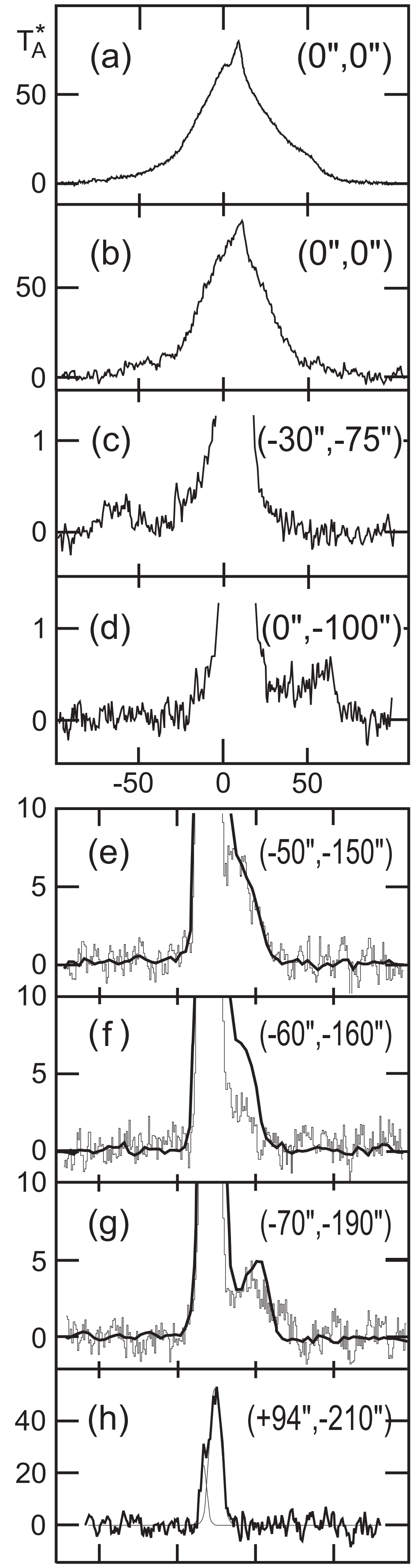

T_A^*
(a)
(0",0")
(b)
(0",0")
(c)
(-30",-75")
(d)
(0",-100")
(e)
(-50",-150")
(f)
(-60",-160")
(g)
(-70",-190")
(h)
(+94",-210")
VELOCITY (km s^{-1})

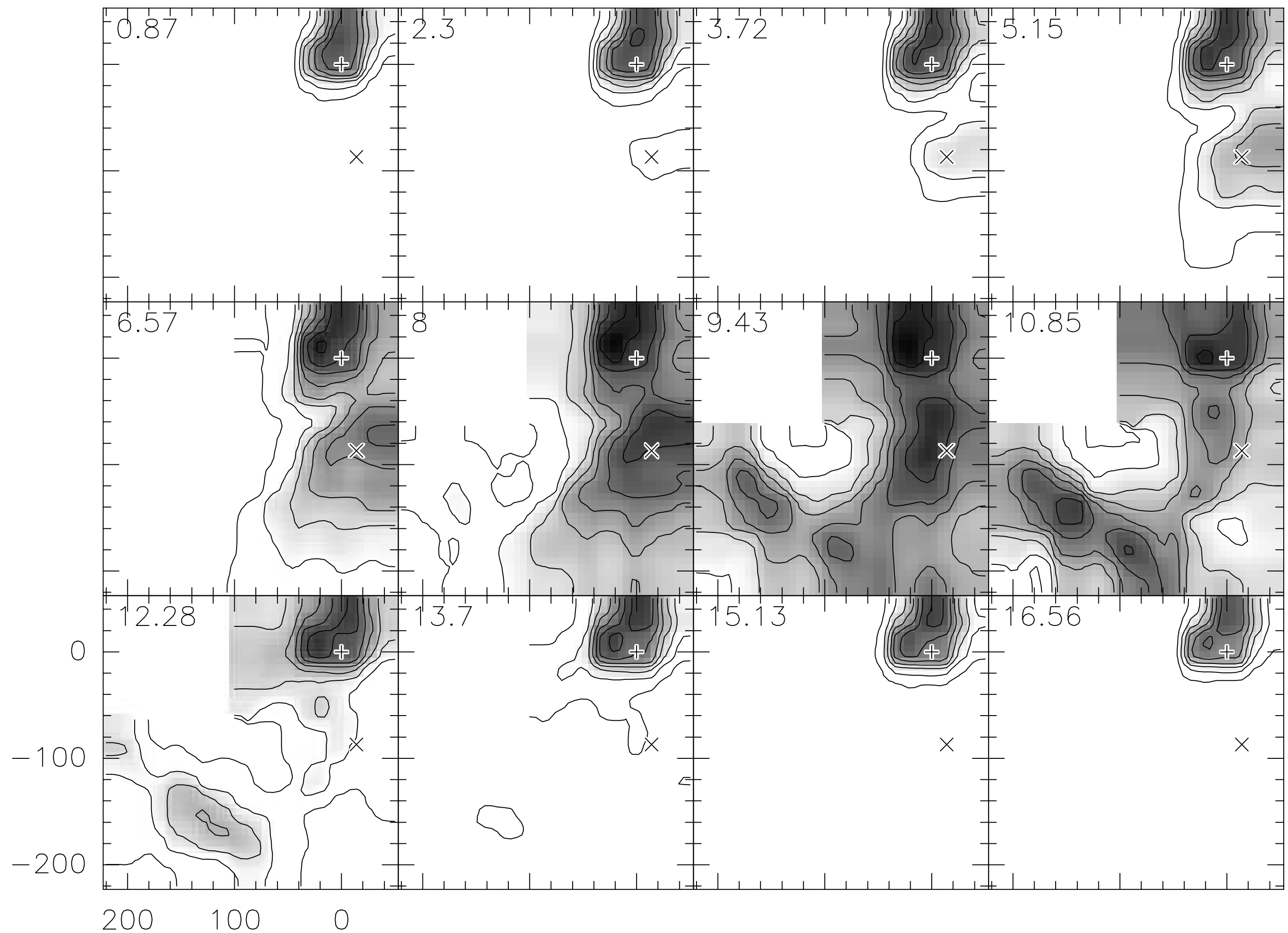

0.87
2.3
3.72
5.15
6.57
8
9.43
10.85
12.28
13.7
15.13
16.56
0
−100
−200
200
100
0

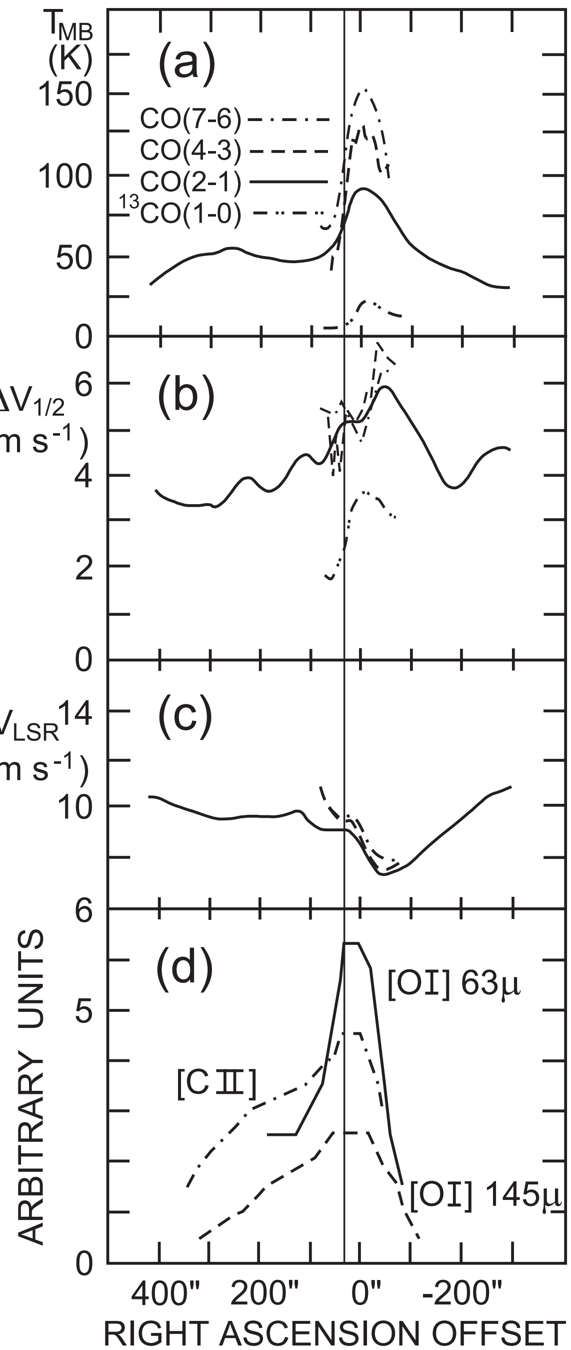

T_MB (K)
(a)
150
100
50
0
CO(7-6)
CO(4-3)
CO(2-1)
13CO(1-0)
ΔV1/2 (km s-1)
(b)
6
4
2
0
V_LSR (km s-1)
(c)
14
10
6
ARBITRARY UNITS
(d)
5
0
[OI] 63μ
[CII]
[OI] 145μ
400"
200"
0"
-200"
RIGHT ASCENSION OFFSET

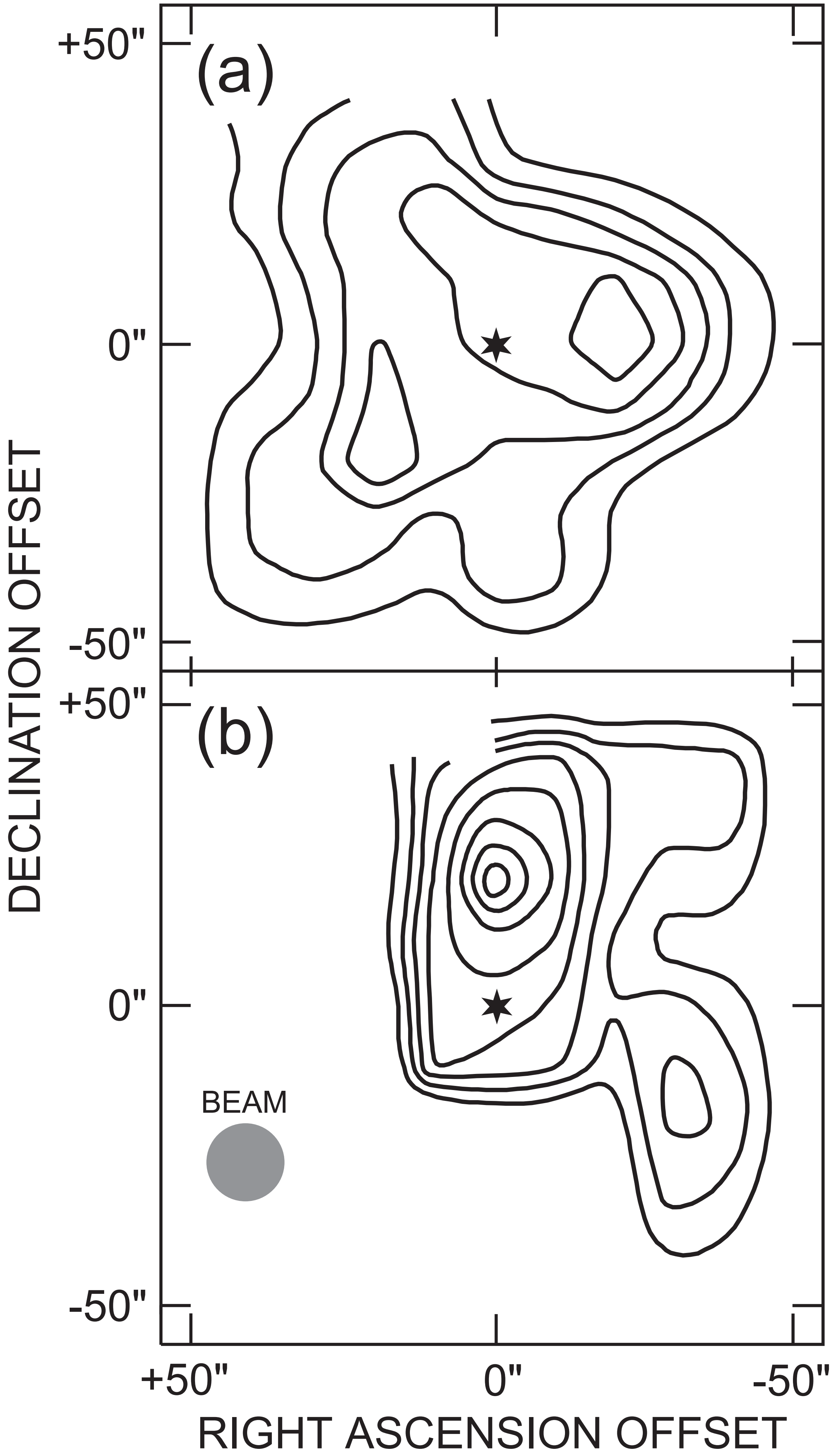

+50"
(a)
0"
-50"
+50"
(b)
0"
BEAM
-50"
+50"
0"
-50"
DECLINATION OFFSET
RIGHT ASCENSION OFFSET

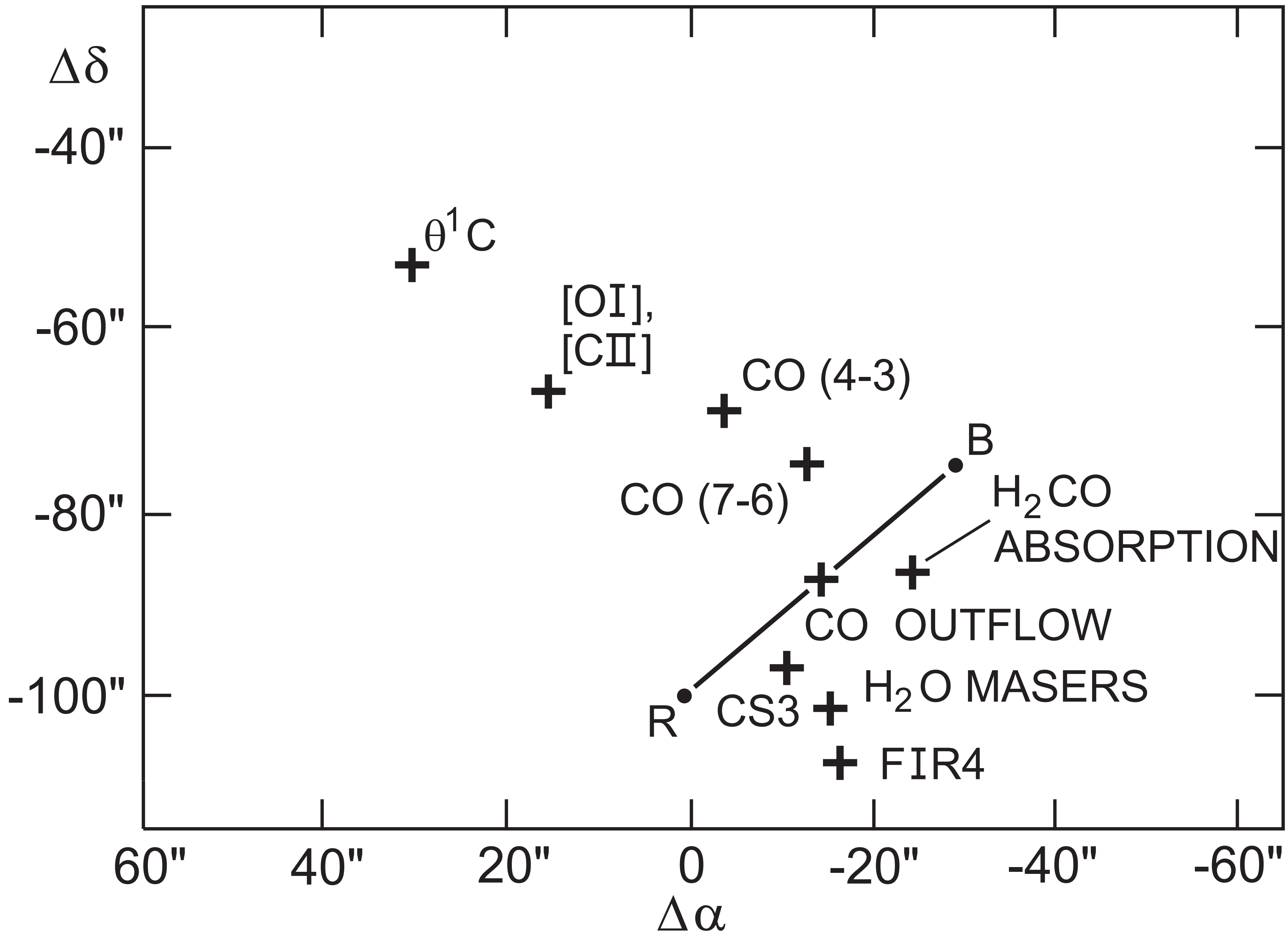

Δδ
-40"
-60"
-80"
-100"
θ¹C
[OI],
[CII]
CO (4-3)
CO (7-6)
B
H₂CO
ABSORPTION
CO OUTFLOW
H₂O MASERS
CS3
R
FIR4
60"
40"
20"
0
-20"
-40"
-60"
Δα

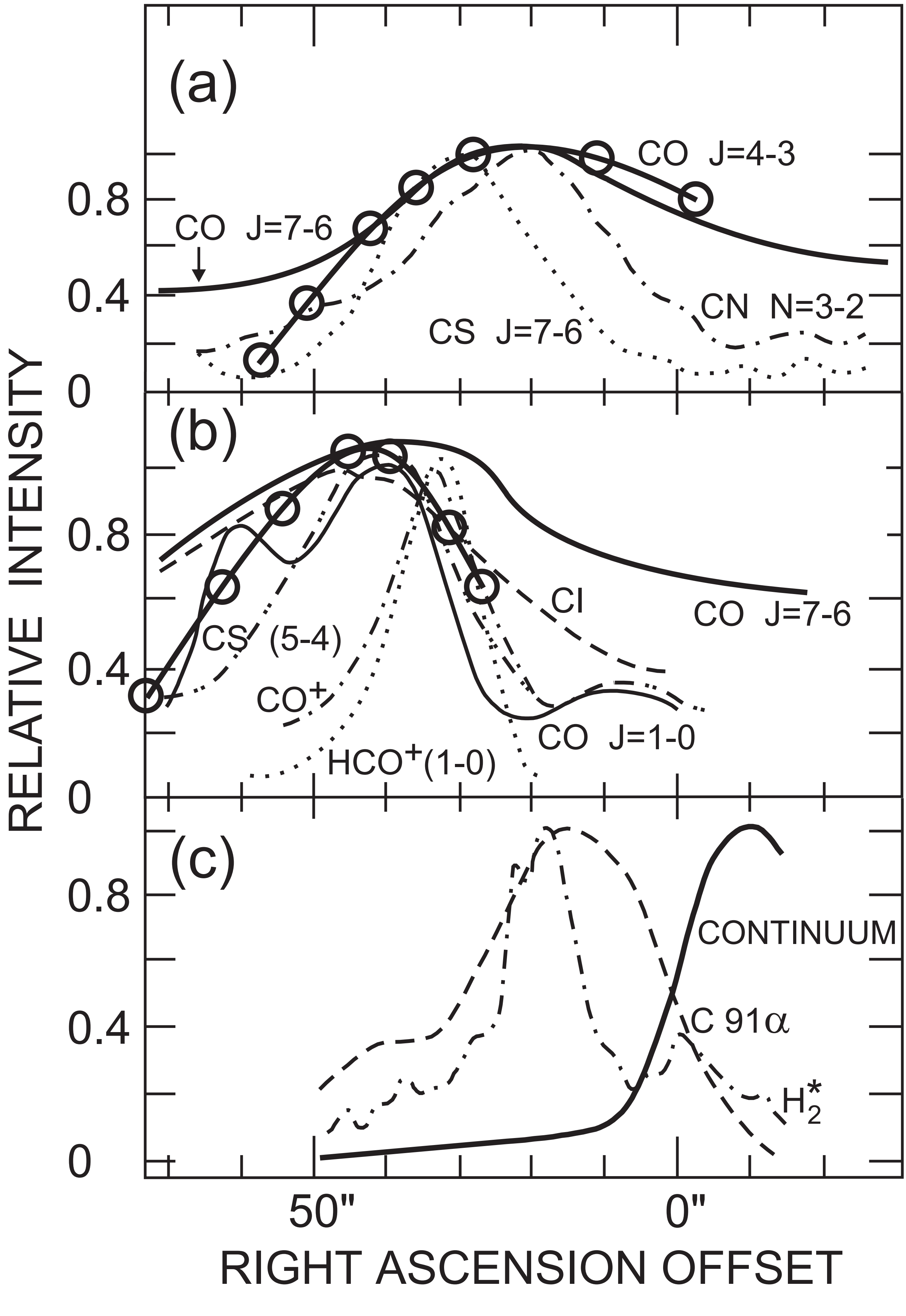

(a)
CO J=4-3
CO J=7-6
CN N=3-2
CS J=7-6
(b)
CI
CO J=7-6
CS (5-4)
CO+
CO J=1-0
HCO+(1-0)
(c)
CONTINUUM
C 91α
H2*
0
0.4
0.8
RELATIVE INTENSITY
50"
0"
RIGHT ASCENSION OFFSET